



## Phase-field modeling of stress generation in polycrystalline LiCoO<sub>2</sub>

Shunsuke Yamakawa<sup>a,\*</sup>, Naoyuki Nagasako<sup>a</sup>, Hisatsugu Yamasaki<sup>b</sup>, Toshiyuki Koyama<sup>c</sup>,  
Ryoji Asahi<sup>a</sup>

<sup>a</sup> Toyota Central R&D Labs., Inc., Nagakute, Aichi 480-1192, Japan

<sup>b</sup> Battery Material Engineering & Research Division, Toyota Motor Corporation, Susono, Shizuoka 410-1193, Japan

<sup>c</sup> Graduate School of Engineering, Nagoya University, Nagoya, Aichi 464-8603, Japan



### ARTICLE INFO

#### Keywords:

Phase-field modeling  
Lithium-ion rechargeable battery  
Polycrystalline secondary particle  
Intercalation-induced stress

### ABSTRACT

The lithium (Li) intercalation process in layered transition-metal oxides is treated as a fundamental phenomenon that affects the battery performance. To gain a quantitative assessment of the influence of the microstructure on the stress generated during the charging process of a polycrystalline secondary particle of Li<sub>x</sub>CoO<sub>2</sub>, the phase-field model considers the crystallographic anisotropies of the Li self-diffusion coefficient and elastic property. Furthermore, the fracture surface ratio of the grain boundary (GB) is evaluated based on the estimated stress distribution over the microstructure. The criteria for crack initiation are obtained such that the maximum principal stress at the GB exceeds the instability criterion,  $\sigma_f$ , of the theory in the linear elastic fracture mechanics. The simulation results show that the stress distribution within polycrystalline Li<sub>x</sub>CoO<sub>2</sub> affects the Li concentration distribution and the phase separation. During the first charging process in the range of  $0.51 \leq x \leq 1.0$  (Li<sub>x</sub>CoO<sub>2</sub>), the total fraction of the fracture surface of the GB is predicted to be < 30% when in the most brittle state and  $\sigma_f$  is 0.5 GPa. Thus, the first charging process results in a nontrivial change to the internal microstructure.

### 1. Introduction

Lithium (Li) transition-metal oxides are commonly used as the positive electrode materials for Li-ion batteries (LIBs) [1–4]. They must allow topotactic electrochemical reactions in order to yield batteries for high power applications [5]. To design the materials for highly improved performance, an accurate and detailed understanding of the Li-ion conduction mechanism at the nanometer to micrometer scale is necessary. The rational design of active electrode materials with higher performance is achieved by an accurate and detailed comprehension of the Li-ion diffusion mechanism at the micrometer scale. Because it is difficult to assess the conduction mechanism experimentally, the details of the influence of microstructure on Li-ion diffusion is not clear yet and comprehensively understood for practical electrode microstructures.

Experimental observations [6] have suggested that the secondary particles include a number of grain boundaries and the primary particles of the secondary particles are not completely isolated, and the surface is not completely exposed to the electrolyte. In the case of LiCoO<sub>2</sub>, the layer-by-layer structure along the *c*-axis is coincident with the Co-O bonding layer, and the first Li occupied layer is a crystallographic feature of LiCoO<sub>2</sub> [7]. The crystallographic lattice constants vary according to the Li concentration, which is especially prominent in

the direction of the *c*-axis. In the case of LiCoO<sub>2</sub>, the *c*-axis lattice constants increase as the Li concentration decreases, ranging from the stoichiometric concentration of  $x = 1.0$  to  $x = 0.5$  in Li<sub>x</sub>CoO<sub>2</sub>. On the other hand, the variations in the lattice constants of the *a*- and *b*-axes are not so significant in comparison with that of the *c*-axis because the octahedral CoO<sub>6</sub> bonding determines the structure of these directions, of which the lattice constants decrease only slightly as the Li concentration decreases. As mentioned above, there is a significant crystallographic anisotropy on the variation of the lattice constants depending on the Li concentration. The crystallographic deterioration of the primary particles within a secondary particle is induced by Li intercalation/deintercalation. Because LiCoO<sub>2</sub> is a brittle material [8,9], stress generation leads to crack propagation between primary particles. The direct observation of crack formation at the grain boundary in polycrystalline LiCoO<sub>2</sub> during the charging process, which leads to a nontrivial change in the microstructure, is reported in Ref. [9]. In a commercially available liquid-state LIB, the electrolyte that intrudes into the crack within a secondary particle can provide active electrochemical reaction interface area between the electrolyte and the active material. On the other hand, in the case of an all-solid-state battery using inorganic solid electrolytes, which have recently attracted considerable interest because of their favorable features, including a lack of

\* Corresponding author.

E-mail address: [e1044@mosk.tytlabs.co.jp](mailto:e1044@mosk.tytlabs.co.jp) (S. Yamakawa).

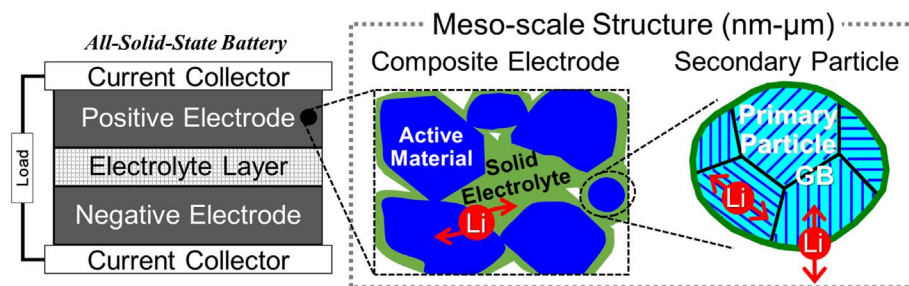


Fig. 1. Schematic illustration of a positive electrode in an all-solid-state LIB.

electrolyte leakage, wide electrochemical window, and high thermal stability [10–14], it is imagined that the particles of the active material are isolated, and the particle surface is not in contact with the electrolyte on the propagation of internal cracks. Even when the liquid-state LIB, increase in the impedance could not be avoidable. Therefore, fundamental information about the mechanical degradation is needed to provide optimized microstructures that resist the capacity fading induced by the charging/discharging process.

The objective of the present study is to estimate the stress generated in a polycrystalline secondary particle of  $\text{LiCoO}_2$  during the first charging process by using a newly developed numerical calculation technique. Multi-scale characteristics of the positive electrode in an all-solid-state battery are illustrated in Fig. 1. The mechanical degradation discussed is primarily related to chemical expansion and phase transformation that occurs with decreasing Li concentration. To this end, we propose an integrated calculation method that enables numerical simulation of Li diffusion in a realistic electrode microstructure. To construct the thermodynamically-consistent model of Li diffusion, we have taken advantage of the phase-field model [15,16], in which the temporal change of the microstructure in the direction of decreasing a free-energy function is calculated. This method has also been used to represent Li diffusion in phase separation [17] and solid solution systems [18]. Moreover, numerical simulations that adopted an isotropic particle model and linear Fickian diffusion-induced stress inside  $\text{LiCoO}_2$  particles were performed utilizing a FIB–SEM-reconstructed  $\text{LiCoO}_2$  half-cell image [19] and the porous electrode along with the pseudo-2D model [20]. Previously [21], we applied the phase-field model to express Li diffusion in the polycrystalline  $\text{LiCoO}_2$  particle. An evaluation of the elastic stress generation coupled with the variation in Li concentration was performed for particular particle morphologies assuming the isotropic elasticity of  $\text{LiCoO}_2$ . To capture important aspects of the influences of the randomly oriented polycrystalline microstructure on the Li mobility and stress generation, introducing the anisotropy of diffusion media and mechanical properties is essential. On the other hand, the quantitative assessment of anisotropic elastic constants is essential for their precise estimation. To date, no reliable experimental stiffness tensors have been reported. Wang et al. only reported the bulk modulus of  $\text{LiCoO}_2$  using a high-pressure experiment [22]. Meanwhile, the theoretically estimated stiffness tensors of  $\text{LiCoO}_2$ , calculated using the lattice mechanics method [23] or the stiffness tensors of  $\text{CoO}_2$  and  $\text{LiCoO}_2$  calculated using density functional theory [24] are available. Wu et al. reported the anisotropic mechanical properties of  $\text{Li}_x\text{CoO}_2$  ( $x = 0.0, 0.5, 0.75, 1.0$ ) [25]. However, the changes in stiffness tensor for each Li concentration were not explicitly explained in Ref. [25]. Although the lattice constant of the  $c$ -axis increases almost continuously as the Li concentration decreases continuously from 1.0 to 0.4, the lattice constant begins to decrease as the Li concentration decreases further. Therefore, it is not obvious whether the linear interpolation between  $\text{CoO}_2$  and  $\text{LiCoO}_2$  for the elastic modulus tensor can be applied or not. Unfortunately, the stiffness tensors of the intermediate state have not been reported. Therefore, we also conduct a first-principles examination of the estimation of the stiffness tensors of  $\text{Li}_x\text{CoO}_2$  ( $x = 0.5, 0.75, 1.0$ ).

The outline of this paper is as follows. In Section 2, the main characteristics of the simulation methods used to model the distribution of Li concentration, elastic stress, and the crack propagation are described. In Section 3.1, the elastic constants of  $\text{Li}_x\text{CoO}_2$  obtained by using density functional calculations are summarized. The practical applications are illustrated using a bi-crystal model (in Section 3.2), a 2D polycrystalline thin film (in Section 3.3), and secondary particle (in Section 3.4), and the dependence of stress generation on the Li concentration on the microstructures is discussed. We also applied the phase-field model to investigate the crack propagation in particulate polycrystalline  $\text{Li}_x\text{CoO}_2$  during the first charging process. The conclusions are given in Section 4.

## 2. Numerical calculation method

### 2.1. Diffusion equation including elastic strain energy

In order to represent anisotropic Li diffusion, the diffusion equation of Cahn–Hilliard type is used [18].

$$\frac{\partial c}{\partial t} = \nabla \cdot \left[ \frac{c(1-c)}{RT} \mathbf{D}' \cdot \nabla \frac{\delta G_{\text{system}}}{\delta c} \right] \quad (1)$$

Here,  $c$  is the local concentration ratio of Li compared to the maximum Li concentration,  $c_{\text{Li}}^{\text{max}}$ , so that it has a value between 0 ( $\text{CoO}_2$ ) and 1 ( $\text{LiCoO}_2$ ). This variable  $c$  corresponds to  $x$  in  $\text{Li}_x\text{CoO}_2$ . The coefficient  $R$  is the gas constant, and  $T$  is the absolute temperature. Eq. (1) was numerically solved using the finite volume method under periodic boundary conditions. Microstructural characteristics were reflected in the components of the diffusion tensor,  $D'_{ij}(\mathbf{r})$ . In the grain interior,  $D'_{ij}(\mathbf{r})$  is represented in the following form:

$$D'_{ij}(\mathbf{r}) = A_{im}(\mathbf{r}) A_{jn}(\mathbf{r}) \delta_{mn} D_{mn}. \quad (2)$$

Here, we assumed planar isotropy of Li diffusion on the hexagonal basal plane of  $\text{LiCoO}_2$ . The variables  $D_{11}$  ( $=D_{22}$ ) and  $D_{33}$  correspond to  $D_{\text{self,basal}}$  and  $D_{\text{self,c-axis}}$ , respectively, where  $D_{\text{self,basal}}$  and  $D_{\text{self,c-axis}}$  are the self-diffusion coefficients in the direction along the hexagonal basal plane and perpendicular to the basal plane, respectively. The coefficient  $\delta_{mn}$  is the Kronecker delta. In this case of a two-dimensional polycrystalline microstructure, the rotation matrix,  $A_{ij}(\mathbf{r})$ , is uniquely determined by the orientation angle, which is randomly assigned for each grain:

$$(A_{ij}) = \begin{pmatrix} \cos \theta & -\sin \theta & 0 \\ \sin \theta & \cos \theta & 0 \\ 0 & 0 & 1 \end{pmatrix}. \quad (3)$$

To consider the effects of the elastic strain energy, the total free energy  $G_{\text{system}}$  is expressed as

$$G_{\text{system}} = G_{\text{chem}} + E_{\text{grad}} + E_{\text{str}}, \quad (4)$$

where  $G_{\text{chem}}$ ,  $E_{\text{grad}}$ , and  $E_{\text{str}}$  mean the chemical part of the free energy, gradient energy, and elastic strain energy, respectively.  $G_{\text{chem}}$  is determined by

Download English Version:

<https://daneshyari.com/en/article/7744470>

Download Persian Version:

<https://daneshyari.com/article/7744470>

[Daneshyari.com](https://daneshyari.com)